

Chiral halogen and chalcogen bonding receptors for discrimination of stereo- and geometric dicarboxylate isomers in aqueous media

Received 00th January 20xx,
Accepted 00th January 20xx

DOI: 10.1039/x0xx00000x

Jason Y. C. Lim^a, Igor Marques^b, Vítor Félix^b and Paul. D. Beer^{*a}

www.rsc.org/

Novel chiral halogen and chalcogen bonding receptors exhibit different selectivities for stereo- and geometric dicarboxylate isomers compared to a hydrogen bonding analogue. The unique geometric and electronic properties of the chalcogen bonding receptor facilitate the diagnostic fluorescence sensing of geometric dicarboxylate isomer guest species.

Dicarboxylates are an important class of anions, being key intermediates in a number of fundamental biological processes including metabolism (e.g. fumarate, glutarate)¹ and signal transduction (e.g. aspartate, glutamate),^{2,3} as well as being crucial intermediates in manufacturing (e.g. phthalates)⁴ and pharmaceutical industries (e.g. tartrate, adipate).⁵ Their pervasiveness stems from the structural diversity of the spacer units between their anionic termini, which can possess a range of functional groups (e.g. amine, keto or hydroxyl) and exist as different stereo- (e.g. tartrate, glutamate) or geometric isomers (e.g. *E/Z*-alkenes of fumarate/maleate). These small structural differences often translate to dramatically contrasting bioactivities.^{6,7} Hence, abiotic receptors capable of selectively binding and sensing target dicarboxylate guest species over structurally-related analogues are highly sought-after.⁸ A diverse range of polytopic host molecules have been reported for dicarboxylate recognition which rely on hydrogen bonding (HB)^{9–11} and coordination with Lewis acidic main group elements,¹² transition metals^{13,14} and f-block elements.^{15,16}

In recent years, σ -hole interactions such as halogen (XB) and chalcogen bonding (ChB) are emerging as powerful complementary interactions to the ubiquitous HB for anion recognition.¹⁸ Arising from the anisotropic distribution of electron density on heavy polarisable Group 16/17 donor atoms, the resulting ChB/XB interactions with Lewis bases exhibit more stringent linearity compared with HB,^{19–22} and

often show superior binding affinities towards anions.^{23,24} Importantly, XB and ChB donors possess subtle geometric, steric and electronic differences which can potentially be exploited to influence selectivity. For instance, divalent ChB donor atoms can possess up to two σ -holes compared to only one for monovalent XB donors, and possess greater steric bulk due to the presence of a second substituent to satisfy the chalcogen atom's valency requirements. Capitalising on these differences, herein we describe the synthesis of a series of chiral XB, ChB[†] and HB receptors (Figure 1) and demonstrate their contrasting abilities to discriminate between stereo- and geometric dicarboxylate isomers for the first time. In addition, each receptor exhibits highly characteristic fluorescence sensory responses to different geometric dicarboxylate isomers, highlighting the potential of σ -hole interactions in anion sensor development.

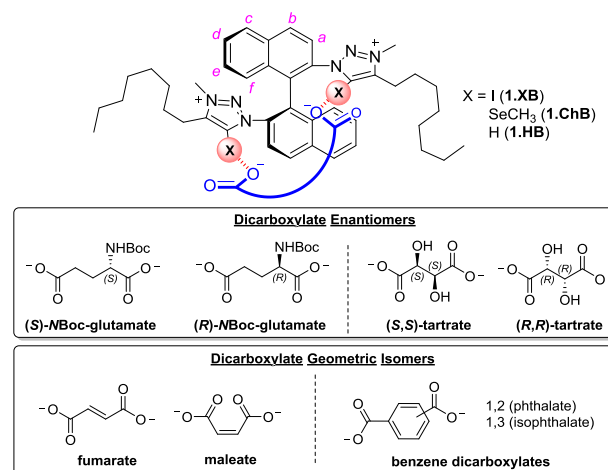


Figure 1. Structure and proposed ditopic dicarboxylate binding mode of receptors **1.HB/ ChB/ XB**, together with the guest dianions studied.

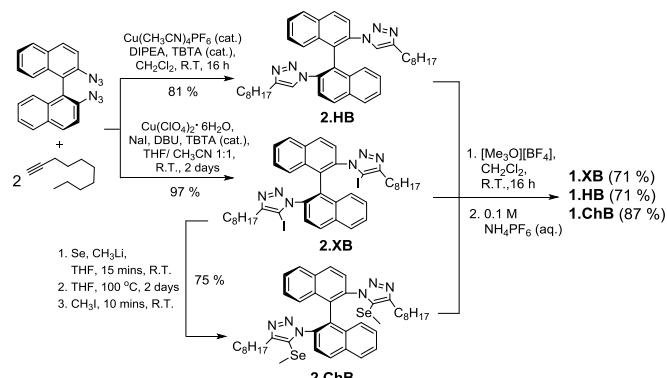
The synthesis of the target receptors is summarised in Scheme 1. (*S*)-Binaphthyl-2,2'-bis(azide), synthesised from enantiopure (*S*)-1,1'-binaphthyl-2,2'-diamine (BINAM),²⁵ was reacted with two equivalents of 1-decyne under copper(I)-

^a Chemistry Research Laboratory, Department of Chemistry, University of Oxford, Mansfield Road, Oxford, OX1 3TA, UK. E-mail: paul.beer@chem.ox.ac.uk.

^b Department of Chemistry, CICECO – Aveiro Institute of Materials, University of Aveiro, 3810-193, Aveiro, Portugal.

Electronic Supplementary Information (ESI) available: Synthesis, structural characterisation, binding studies details, computational methods, and additional figures and tables

catalysed azide-alkyne cycloaddition (CuAAC) conditions to afford neutral precursors **2.HB** and **2.XB**. Nucleophilic S_NAr substitution reaction of excess $LiSeCH_3$ with **2.XB** afforded **2.ChB**.[‡] Bis-methylation of the neutral precursors using trimethyloxonium tetrafluoroborate followed by anion exchange to the non-coordinating PF_6^- salts produced the target dicationic receptors **1.XB**, **1.ChB** and **1.HB**.



Scheme 1. Synthesis of receptors **1.XB**, **1.ChB** and **1.HB**.

The receptors' dicarboxylate anion binding properties were investigated by 1H NMR titration experiments in d_6 -acetone/ D_2O 85:15 v/v. The addition of dicarboxylate tartrate and NBoc-glutamate enantiomers (as their TBA salts) generally elicited similar patterns of perturbations in each receptor's aromatic proton resonances (see Section S3, ESI). Notable downfield shifts of the H_b signals (assignment in Fig. 1) were seen in all cases, possibly arising from weak HB interactions with the anions bound in close proximity by the triazoliums, whilst proton signals from H_d , H_e and H_f located further from the binding site moved upfield. In comparison, the dicarboxylate geometric isomers elicited more varied signal shifts. For example, although H_b shifted the most for **1.ChB** and **1.HB** upon phthalate addition, H_f was perturbed most prominently during the isophthalate titrations. Contrastingly, the largest shifts were observed for H_f when both benzene dicarboxylates were added to **1.XB**. With different enantiomers or geometric isomers, notable differences in the shapes of the resulting binding isotherms for either H_b or H_f were seen, showing that all receptors could discriminate between different dicarboxylate guests. BindFit²⁶ analysis of the 1H NMR titration data determined in general 1:2 host-guest stoichiometric association constants (K/M^{-1}) (values shown in Tables S3-1, ESI). In every case, the value of K_{11} was larger than K_{12} by at least an order of magnitude, indicating that the second anion guest is interacting weakly with the bound complex. Taking this into account, only the K_{11} values (summarised in Fig. 2 pictorially) were considered to quantify the extent of dicarboxylate isomer discrimination (numerical values in Table S3-2, ESI).

Importantly, the influences of the charge-assisted σ -hole interactions on both chiral and geometric isomer dicarboxylate anion selectivity are evident from Figure 2. Amongst the receptors, **1.XB** showed the greatest degree of enantioselectivity, with tartrate better discriminated than NBoc-glutamate possibly due to the presence of more chiral

centres enforcing a greater structural difference between isomers. By contrast, **1.ChB** displayed poor chiral selectivity. Notably, both σ -hole donors showed augmented geometric isomer discrimination relative to **1.HB**. With the benzene dicarboxylates, the selectivity of both **1.XB** and **1.ChB** for isophthalate over phthalate greatly surpassed that of **1.HB**. It is noteworthy that **1.ChB** exhibited enhanced fumarate/maleate discrimination ($K_{fum}/K_{mal} = 5.5 \pm 0.2$) compared with **1.HB** ($K_{fum}/K_{mal} = 2.0 \pm 0.1$), while **1.XB** was unstable to maleate, preventing quantification of fumarate/maleate selectivity. The greater stability of **1.ChB** to highly basic anions may render ChB hosts valuable alternatives to XB for recognition and sensing.

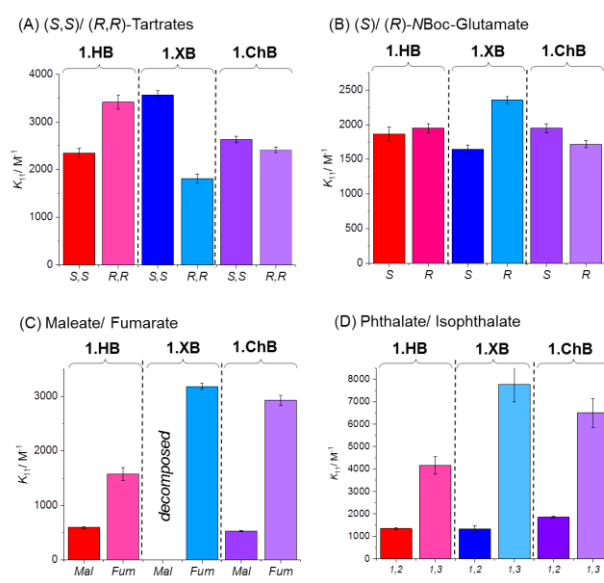


Figure 2. Bar charts showing the variations in K_{11}/M^{-1} values between dicarboxylate (A, B) enantiomers and (C, D) geometric isomers for receptors **1.XB**, **1.ChB** and **1.HB**, determined from 1H NMR titration experiments ($[host] = 1.0$ mM, d_6 -acetone/ D_2O 85:15 v/v, $T = 298$ K).

The electronic and steric properties of each receptor's binding site were probed with DFT calculations using models **1.HB_{Me}**, **1.ChB_{Me}** and **1.XB_{Me}** containing methyl groups instead of octyl chains and employing the ω B97X functional and the 6-311++G(d,p) basis set for all atoms apart from iodine (aug-cc-pVDZ-PP) and selenium (aug-cc-pVDZ) (full details in Section S5.3, ESI). The locations of the σ -holes of iodine and selenium donor atoms in **1.XB_{Me}** and **1.ChB_{Me}** are shown in Fig. S5-2, ESI. Although the most positive electrostatic potential (V_S) values within each receptor's binding cleft decrease in the order **1.HB_{Me}** > **1.XB_{Me}** > **1.ChB_{Me}** (see Table S5-1, ESI), for **1.HB_{Me}** the positive potential region is widespread, allowing many possible nondirectional interactions compared to the more localised positive potentials of **1.XB_{Me}** and **1.ChB_{Me}**. Despite the different donor groups (H, $SeCH_3$, I) present, the conformations of all three receptors are similar, with both triazolium units oriented nearly antiparallel with each other and perpendicular to the adjacent naphthyl aromatic moieties. Moreover, these rings are twisted around the C-C

interannular bond by comparable $C_{\text{naphthyl}}-C-C-C_{\text{naphthyl}}$ torsion angles (α angle) of 91.5, 89.4 and 90.3° for **1.XB_{Me}**, **1.ChB_{Me}** and **1.HB_{Me}** respectively. Notably, the bulky methyl groups of SeCH₃ on **1.ChB_{Me}** are oriented away from each other to minimise steric hindrance, whilst also giving a separation between the positions of the σ -holes (6.505 Å), which is *ca.* 0.1 Å longer than in **1.XB_{Me}** (6.370 Å).

To compare the host-guest binding conformations for each receptor with the tartrate enantiomers and benzene dicarboxylate geometric isomers, molecular dynamics (MD) simulations were performed with AMBER16²⁷ using the General Amber Force Field (GAFF)^{28,29} in periodic cubic boxes containing 627 and 871 randomly-distributed water and acetone molecules respectively (acetone/ water 85:15 v/v) (see Section S5.3, ESI). The σ -holes on **1.XB** and **1.ChB** were described using the extra-point of charge approach and the host-guest interactions between the three receptors and the carboxylate groups in the MD simulation were maintained using suitable distance and angle restraints. For the benzene dicarboxylates, where the most negative V_s values were situated at the COO⁻ groups (Fig. S5-1, ESI), both host donor atoms could interact monotonically with a single COO⁻ group (scenario A) (Fig. 3 and S5-3, ESI) or with individual oxygen atoms on separate COO⁻ moieties (scenario B) (Fig. 3 and S5-3, ESI). For the tartrate enantiomers, the most negative V_s values located near the hydroxyl groups (Fig. S5-2, ESI) led to binding scenarios where the receptors could establish two interactions with individual COO⁻ groups (scenario B) or hydroxyl groups (scenario C) (Fig. S5-4, ESI). The guest geometry appears to influence the receptors' conformations to a small extent (see Section S5.2, ESI) regardless of binding scenario. While monotopic guest binding in scenario A results in no significant changes in the inter-triazolium $z \cdots z$ distances ($z = I/Se/H$) and α angles as expected, ditopic binding in scenario B leads to a slight increase in the $z \cdots z$ distances between phthalate and isophthalate, mirroring the DFT-computed intramolecular inter-COO⁻ distance of each anionic isomer (phthalate: 3.964 Å; isophthalate: 6.142 Å). Notably, the latter dimensions are comparable to the distances between the σ -holes in **1.XB_{Me}** and **1.ChB_{Me}**, suggesting good size and geometric complementarity. Receptor conformation was found to be independent of the tartrate enantiomers due to their flexible aliphatic structures enabling them to undergo considerable conformational changes throughout the MD simulations when bound.

The limited conformational changes of the receptors' rigid structural framework in the presence of different dicarboxylates emphasises the importance of their respective interactions' directionality in determining guest selectivity. The DFT calculations showed that the location of the σ -holes on **1.ChB** is less well-defined than in **1.XB** (*vide supra* and Section S5.3, ESI). Thus, despite the use of geometrical restraints when simulating the host-guest interactions, the ChB interactions show less stringent linearity than XB, as apparent from the slightly larger standard deviations of the C-Se \cdots O₂C⁻ angles as compared to C-I \cdots O₂C⁻ (see Table S5-3, ESI). Importantly, the poor linearity of the HB interactions from **1.HB** allows the

dicarboxylate guests to adopt a large range of binding arrangements (Fig. S5-4 ESI), reducing the ability of the host to discriminate between them.

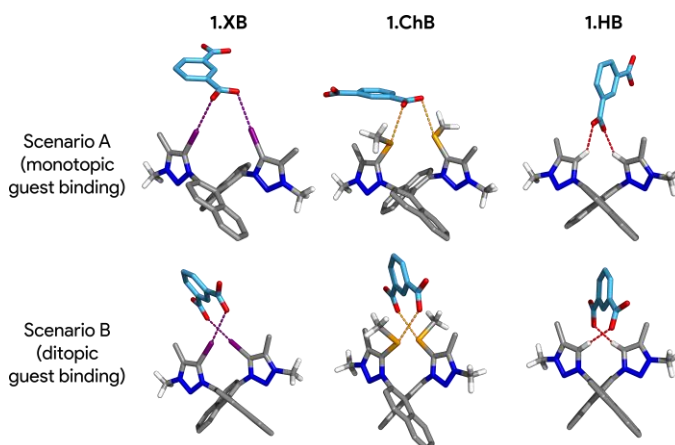


Figure 3. Illustrative MD snapshots of the isophthalate complexes of **1.XB**, **1.ChB** and **1.HB** in scenarios A and B. The XB, ChB and HB interactions are depicted as purple, orange and red dashed lines, respectively. The octyl chains are replaced with methyl groups and the solvent molecules and most hydrogen atoms were hidden for clarity.

Having established the roles of each interaction for oxoanion binding, the fluorescence dicarboxylate anion sensing properties of the receptors were then investigated in acetone/H₂O 85:15 v/v (Section S4, ESI). The addition of all anions⁵ resulted in large enhancements of the **1.XB** receptor's fluorescence intensity, possibly resulting from modulation of the intramolecular heavy-atom effect due to the XB-donor iodine atoms interacting with the anion guest species,^{30,31} concomitant with notable bathochromic shifts of **1.XB**'s maximum emission wavelength (λ_{em}) (Fig. 4A). With **1.HB**, all anions elicited significant fluorescence quenching with the λ_{em} unchanged in all cases except for isophthalate, which showed a hypsochromic shift. In comparison, **1.ChB** displayed unique fluorescence intensity responses and λ_{em} changes upon binding different dicarboxylate anions (Fig. 4B). Compared with **1.XB**, the greater stability of **1.ChB** to anions and more varied fluorescent responses renders this σ -hole receptor potentially more useful for optical sensory guest discrimination.

In summary, a family of chiral XB, ChB and HB host systems have been synthesised which display contrasting selectivity and fluorescence sensing behaviour towards dicarboxylate stereo- and geometric isomers arising from their unique geometric and electronic properties. Whilst **1.XB** exhibited the best stereoselectivity, both **1.XB** and **1.ChB** displayed augmented discrimination for dicarboxylate geometric isomers compared to **1.HB**, dictated by more prominent directionality and better host-guest size and geometric complementarity as demonstrated through MD simulations. It is noteworthy that **1.ChB** displayed diagnostic fluorescence responses to different dicarboxylate geometric isomers and enhanced stability towards highly basic oxoanions in aqueous solvent media. These valuable traits highlight the unique potential of ChB to

complement XB and HB for future sensor development towards biologically- and industrially-relevant oxoanions in diverse medical, environmental and analytical applications.

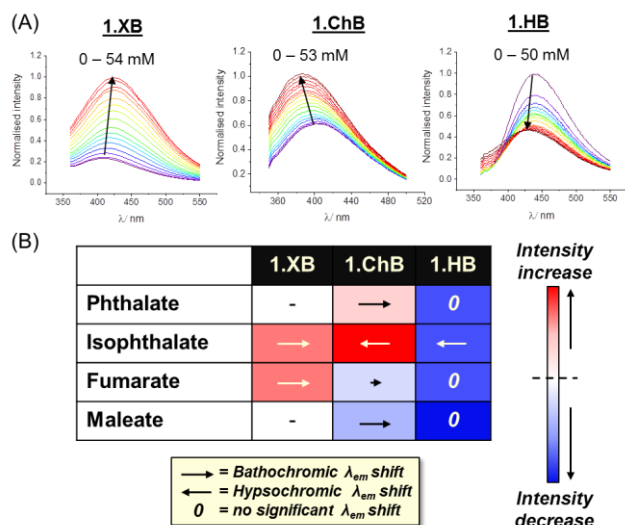


Figure 4. (A) Fluorescence spectra of receptors (A) **1.XB** (λ_{ex} = 325 nm), (B) **1.HB** (λ_{ex} = 330 nm) and (C) **1.ChB** (λ_{ex} = 320 nm) in the presence of increasing quantities of isophthalate, with concentrations indicated. (B) Summary chart of the fluorescence intensity changes and λ_{em} shifts for each receptor with different dicarboxylate geometric isomers. The length of each arrow denotes the magnitude of λ_{em} shift while the shade of red/blue indicates the extent of fluorescence change from 0 to 20 mM of guest ([host] = 50 μ M; acetone/ H₂O 85:15 v/v, T = 293 K).

Conflicts of interest

There are no conflicts of interest to declare.

Acknowledgements

J.Y.C.L. acknowledges the Agency for Science, Technology and Research (A*STAR), Singapore, for postgraduate research funding. The theoretical studies were supported by projects P2020-PTDC/QEQ-SUP/4283/2014 and CICECO – Aveiro Institute of Materials (UID/CTM/50011/2013), financed by National Funds through the FCT/MEC and, when applicable, co-financed by QREN-FEDER through COMPETE, under the PT2020 Partnership Agreement.

Notes and references

‡ The Se ChB-donor was prepared rather than the Te analogue due to instability of the cationic methyltelluro-triazolium motif previously observed.²⁴

† C_{naphthyl} are the carbon atoms bonded to the triazolium units.

§ Decomposition of **1.XB** was observed in large excess of maleate and phthalate, preventing reliable fluorescence changes to be discerned following formation of their non-covalent complexes.

1 D. Voet and J. G. Voet, *Biochemistry*, Wiley, New York, 2nd edn., 1995.

- A. Cavallero, A. Marte and E. Fedele, *J. Neurochem.*, 2009, **110**, 924–934.
- S. R. Platt, *Vet. J.*, 2007, **173**, 278–286.
- R. D. Sanderson, D. F. Schneider and I. Schreuder, *J. Appl. Polym. Sci.*, 1994, **53**, 1785–1793.
- A. O. Surov, A. N. Manin, A. P. Voronin, K. V. Drozd, A. A. Simagina, A. V. Churakov and G. L. Perlovich, *Eur. J. Pharm. Sci.*, 2015, **77**, 112–121.
- A. Munnich, *Nat Genet.*, 2008, **40**, 1148–1149.
- S. Eiam-ong, M. Spohn, N. A. Kurtzman and S. Sabatini, *Kidney Int.*, 1995, **48**, 1542–1548.
- D. Curiel, M. Más-Montoya and G. Sánchez, *Coord. Chem. Rev.*, 2015, **284**, 19–66.
- A. M. Costero, M. Colera, P. Gavina and S. Gil, *Chem Commun*, 2006, 761–763.
- R. Gotor, A. M. Costero, P. Gaviña, S. Gil and M. Parra, *Eur. J. Org. Chem.*, 2013, **2013**, 1515–1520.
- A. Ragusa, S. Rossi, J. M. Hayes, M. Stein and J. D. Kilburn, *Chem. – Eur. J.*, 2005, **11**, 5674–5688.
- C. W. Gray and T. A. Houston, *J. Org. Chem.*, 2002, **67**, 5426–5428.
- T. Noguchi, B. Roy, D. Yoshihara, Y. Tsuchiya, T. Yamamoto and S. Shinkai, *Chem. – Eur. J.*, 2014, **20**, 381–384.
- R. J. Motekaitis and A. E. Martell, *Inorg. Chem.*, 1992, **31**, 5534–5542.
- S. E. Plush and T. Gunnlaugsson, *Org. Lett.*, 2007, **9**, 1919–1922.
- S. M. Lacy, D. M. Rudkevich, W. Verboom and D. N. Reinhoudt, *J Chem Soc Perkin Trans 2*, 1995, 135–139.
- J. Y. C. Lim, I. Marques, L. Ferreira, V. Félix and P. D. Beer, *Chem Commun*, 2016, **52**, 5527–5530.
- J. Y. C. Lim and P. D. Beer, *Chem*, 2018, **4**, 731–783.
- L. C. Gilday, S. W. Robinson, T. A. Barendt, M. J. Langton, B. R. Mullaney and P. D. Beer, *Chem. Rev.*, 2015, **115**, 7118–7195.
- G. Cavallo, P. Metrangola, R. Milani, T. Pilati, A. Priimagi, G. Resnati and G. Terraneo, *Chem. Rev.*, 2016, **116**, 2478–2601.
- G. E. Garrett, G. L. Gibson, R. N. Straus, D. S. Seferos and M. S. Taylor, *J. Am. Chem. Soc.*, 2015, **137**, 4126–4133.
- P. C. Ho, P. Szydłowski, J. Sinclair, P. J. W. Elder, J. Kübel, C. Gendy, L. M. Lee, H. Jenkins, J. F. Britten, D. R. Morim and I. Vargas-Baca, *Nat. Commun.*, 2016, **7**, 11299.
- A. Brown and P. D. Beer, *Chem Commun*, 2016, **52**, 8645–8658.
- J. Y. C. Lim, I. Marques, A. L. Thompson, K. E. Christensen, V. Félix and P. D. Beer, *J. Am. Chem. Soc.*, 2017, **139**, 3122–3133.
- Y. Takeda, M. Okazaki and S. Minakata, *Chem Commun*, 2014, **50**, 10291–10294.
- www.supramolecular.org.
- D. A. Case, R. M. Betz, W. Botello-Smith, D. S. Cerutti, I. T. E. Cheatham, T. A. Darden, R. E. Duke, T. J. Giese, H. Gohlke, A. W. Goetz, N. Homeyer, S. Izadi, P. Janowski, J. Kaus, A. Kovalenko, T. S. Lee, S. LeGrand, P. Li, C. Lin, T. Luchko, R. Luo, B. Madej, D. Mermelstein, K. M. Merz, G. Monard, H. Nguyen, H. T. Nguyen, I. Omelyan, A. Onufriev, D. R. Roe, A. Roitberg, C. Sagui, C. L. Simmerling, J. Swails, R. C. Walker, J. Wang, R. M. Wolf, X. Wu, L. Xiao, D. M. York and P. A. Kollman, *AMBER 2016*, University of California, San Francisco, 2016.
- J. Wang, R. M. Wolf, J. W. Caldwell, P. A. Kollman and D. A. Case, *J. Comput. Chem.*, 2004, **25**, 1157–1174.
- J. Wang, R. M. Wolf, J. W. Caldwell, P. A. Kollman and D. A. Case, *J. Comput. Chem.*, 2005, **26**, 114–114.
- M. Rae, F. Perez-Balderas, C. Baleizão, A. Fedorov, J. A. S. Cavaleiro, A. C. Tomé and M. N. Berberan-Santos, *J. Phys. Chem. B*, 2006, **110**, 12809–12814.
- F. Zapata, A. Caballero, P. Molina, I. Alkorta and J. Elguero, *J. Org. Chem.*, 2014, **79**, 6959–6969.